



# Ion-acoustic compressive and rarefactive solitary waves in unmagnetised plasmas with positrons and two-temperature superthermal electrons

P C SINGHADIYA<sup>1</sup>, J K CHAWLA<sup>2,\*</sup> and S K JAIN<sup>3</sup>

<sup>1</sup>Seth RLS Government College, Kaladera 303 801, India

<sup>2</sup>Haridev Joshi Government Girls College, Banswara 327 001, India

<sup>3</sup>Government College, Dholpur 328 001, India

\*Corresponding author. E-mail: jitendra123chawla@yahoo.co.in

MS received 31 October 2019; revised 6 February 2020; accepted 13 February 2020;  
published online 21 May 2020

**Abstract.** Ion-acoustic solitary waves (IASWs) in plasma consisting of ions, positrons and superthermal electrons in two distinct temperatures have been studied. The reductive perturbation method (RPM) has been employed to derive the Korteweg–de Vries and modified KdV equation. Numerical and analytical studies show that compressive and rarefactive solitons exist for the selected parametric range depending on the spectral indexes,  $\kappa$  ( $\kappa_h, \kappa_c$ ) and their respective densities ( $\nu, \mu$ ). It is found that spectral indexes ( $\kappa_h, \kappa_c$ ) and their relative densities have significant impact on the basic properties, i.e., amplitude and width as well as on the nature of IASWs. Variations of amplitude and width for the compressive and rarefactive solitary waves have been analysed graphically with different plasma parameters like spectral indexes of cold and hot electrons ( $k_c, k_h$ ), their respective densities, ionic temperature ratio, positron temperature ratio as well as with the temperature ratio of the two-electron species. The amplitude of the compressive (rarefactive) solitary waves increases (decreases) on increasing  $k_h$ . However, the amplitude of the compressive (rarefactive) solitary waves decreases (increases) on increasing  $k_c$ . The investigations of such solitary waves may be helpful for the critical understanding of space where superthermal electrons with two different temperatures exist along with positrons and ions (e.g. Saturn's magnetosphere, pulsar magnetosphere).

**Keywords.** Solitary wave; reductive perturbation method; Korteweg–de Vries equation; positron and superthermal electron.

**PACS Nos** 52.35.Mw; 52.35.Sb

## 1. Introduction

Ion-acoustic solitary waves (IASWs) have been investigated extensively due to their presence in various astrophysical plasmas, e.g., Earth's auroral region, plasma sheet, Saturn's magnetosphere, pulsar magnetosphere, solar wind [1–4] etc. as well as in laboratory experiments by electron beam [5]. Investigations of IASWs provide a deep understanding of the underlying nonlinear phenomena in plasmas.

The fluid theories for small-amplitude as well as large-amplitude ion-acoustic solitons show that the ion-acoustic rarefactive solitons (IARSs) in a two-electron temperature (TET) plasma exists only for certain density and temperature ratios of the hot and cold electron species [6–18]. This is in broad agreement with the experimental results [19]. However, experimental study

of the IARSs show that there are discrepancies between theoretical predictions and experimental observations [19]. Sayal and Sharma [20] have studied IARSs in a TET plasma considering kinetic effects of electrons and using the fluid equations for cold ions. The properties of dust ion-acoustic Gardner double layers in dusty plasma with two TET have been studied by Masud *et al* [21].

Superthermal (fast and accelerated) particles having high-energy tail in the distribution function are found in various astrophysical and space environments such as Earth's auroral region, plasma sheet, Saturn's magnetosphere, pulsar magnetosphere, solar wind and interstellar medium [22–25]. A large number of measurements in space and astrophysical plasma environments of Saturn's magnetosphere from voyager PLS observations [26,27] and Cassini plasma spectrometer observations [28,29] have shown that the observed waves may be

suitably explained by two-kappa distribution for electrons where the hot component of the superthermal electrons has much lower density than the cold component. Many researchers [27–31] have observed superthermal electrons including hot and cold species having  $\kappa$  distributions  $\kappa_h$  and  $\kappa_c$  in Saturn's magnetosphere.

The behaviour of superthermal electrons observed in astrophysical environment deviates from Maxwellian distribution and found to obey  $\kappa$  distribution. The  $\kappa$  distribution was introduced by Vasyliunas for describing astrophysical plasmas. Hellberg *et al* [32] suggested that the spectral index  $\kappa$  should be greater than 3/2 for superthermal electrons and reduces to Maxwellian distribution as the value of spectral index approaches  $\infty$ . Boubakour *et al* [33] have studied the effect of superthermal electrons and positrons on IASWs in an unmagnetised plasma. El-Tantawy and Moslem [34] studied the large-amplitude ion-acoustic waves in unmagnetised plasma with superthermal electrons and positrons. They have studied the characteristics of solitary and shock waves with different plasma parameters such as spectral indexes of superthermal electrons, positrons, ionic temperature ratio and with dust as well as positron concentration. El-Tantawy *et al* [35] have studied the small-amplitude ion-acoustic structures in dusty plasmas with superthermal electrons. Using reductive perturbation method (RPM), they have derived m-KdV equation. They have studied the effect of superthermal electrons and positrons on the characteristics (amplitude and width) of nonlinear structures. El-Labany *et al* [36] have reported that only large-amplitude compressive IASWs exist in cold negative ion plasma with superthermal electrons having  $\kappa$  distribution. Panwar *et al* [37] have studied the oblique propagation of ion-acoustic cnoidal waves in two-temperature superthermal electrons in magnetised plasma. El-shamy [38] studied the oblique propagation of IASWs in magnetised plasma with superthermal electron and positron using the ZK equation. He found that the characteristics of the solitary waves (e.g. amplitude and width) increase with the increase in the spectral index  $k$ . Alam *et al* [39], in their study of the dust-IASWs in unmagnetised plasma with two-temperature superthermal electron (TTSE) using the RPM, derived KdV, m-KdV and Gardner soliton equations. They found that amplitude of the soliton decreases with an increase in spectral index. Saha *et al* [40] studied the effect of superthermal electrons and positrons on ion-acoustic waves in magnetised plasma using RPM. In their analysis, they found that when spectral index increases, the amplitude of the periodic wave (solitary wave) increases (decreases) and its width increases (decreases). Saini *et al* [41] derived the ZK equation by employing RPM method to study the effect of hot and cold superthermal electrons on IASWs in

a magnetised plasma. Bains *et al* [42] examined the low-frequency ion-acoustic shock waves in magnetised plasma consisting of cold ions and superthermally distributed hot and cold electrons. It is found that the change in temperature ratio and their respective densities play important roles in the properties of solitary waves. The above discussion shows that plasma with TTSEs has been studied by several researchers so far and superthermal parameters drastically affect the nature and properties of the solitons. Therefore, it becomes interesting to study the small-amplitude ion-acoustic solitons in plasma consisting of warm adiabatic ions, hot positrons and TTSEs. Chatterjee *et al* [43] have studied the dust ion-acoustic waves in superthermal electron, using the reductive perturbation technique.

The aim of the present paper is to study the properties of small-amplitude IASWs in plasmas with TTSEs following  $\kappa$  distribution. The effects of spectral indexes along with their respective densities on the properties and nature have been investigated numerically. The paper is organised as follows: in §1, a brief introduction of the superthermal electrons along with their experimental observations and the past studies including their results is given. In §2, using the basic set of hydrodynamic equations governing plasma system and employing RPM, KdV and m-KdV equation have been derived with appropriate boundary conditions. In §3, the exact solutions of the KdV equation has been determined. The m-KdV equation has been derived in §4. Section 5 is devoted to discussion and findings. In §6, conclusions of our investigations have been provided along with potential applications.

## 2. Basic equations

We consider unmagnetised plasma consisting of warm adiabatic ions, hot positrons and superthermal electrons with two-temperature distribution. The governing equations for IASWs in the above described plasma are as follows:

$$\partial_t N + \partial_x(NV) = 0 \quad (1)$$

$$\partial_t V + V\partial_x V = -\partial_x\phi - 2\sigma\partial_x N \quad (2)$$

$$\partial_x^2\phi = n_h + n_c - \alpha n_p - (1 - \alpha)N. \quad (3)$$

The superthermal electrons having two distinct temperatures following  $\kappa$  distribution and positrons may be given by

$$n_c = v \left( 1 - \frac{\phi}{k_c - 3/2} \right)^{-(k_c - 1/2)} \quad (4)$$

$$n_h = \mu \left( 1 - \frac{\sigma_1\phi}{k_h - 3/2} \right)^{-(k_h - 1/2)} \quad (5)$$

$$n_p = e^{-\gamma\phi} = \left(1 - \gamma\phi + \frac{\gamma^2\phi^2}{2} - \frac{\gamma^3\phi^3}{6} + \dots\right). \quad (6)$$

Substituting eqs (4)–(6) in (3), we find

$$\partial_x^2\phi = [1 + \alpha_1\phi + \alpha_2\phi^2] - \alpha n_p - (1 - \alpha)N, \quad (7)$$

where

$$\begin{aligned} \mu &= \frac{n_{c0}}{n_{e0}}, \quad \nu = \frac{n_{h0}}{n_{e0}}, \quad \alpha = \frac{n_{p0}}{n_{e0}}, \\ \alpha_1 &= \frac{(1 - \mu)(2k_c - 1)}{(2k_c - 3)} + \frac{\sigma_1\mu(2k_h - 1)}{(2k_h - 3)}, \\ \alpha_2 &= \frac{(1 - \mu)(4k_c^2 - 1)}{2(2k_c - 3)^2} + \frac{\sigma_1^2\mu(4k_h^2 - 1)}{2(2k_h - 3)^2} \end{aligned}$$

and  $k_{c,h}$  is the  $k$ -distribution corresponding to cold and hot species of electrons.

In the above equations  $N$ ,  $n_p$ ,  $n_c$  and  $n_h$  denote the normalised density of ions, positron, cold and hot electrons, respectively.  $V$  is the normalised fluid velocity of the ions and  $\phi$  is the electric potential.  $\gamma = T_p/T_e$ ,  $\sigma = T_i/T_e$  and  $\sigma_1 = T_c/T_h$  are the ratio of positron and electron temperature, the ratio of ion and electron temperature and the ratio of cold and hot electron temperature respectively. The space coordinate speed ( $x$ ) has been normalised in terms of Debye length speed  $\lambda_D = (\epsilon_0 T_e/n_0 e^2)^{1/2}$  and time coordinates by the inverse of ion plasma frequency.

To derive the KdV equation from the basic set of equations, viz. eqs (1)–(7), we use RPM, by introducing the following stretched coordinates ( $\xi$ ) and ( $\tau$ ) as

$$\xi = \varepsilon^{1/2}(x - St) \quad (8a)$$

and

$$\tau = \varepsilon^{3/2}t, \quad (8b)$$

where  $\varepsilon$  is a small parameter and  $S$  is the phase velocity of the wave, to be determined later.

Now we expand the dependent variables in the following form:

$$\begin{aligned} \begin{bmatrix} N \\ V \\ \phi \end{bmatrix} &= \begin{bmatrix} 1 \\ 0 \\ 0 \end{bmatrix} + \varepsilon \begin{bmatrix} N^{(1)} \\ V^{(1)} \\ \phi^{(1)} \end{bmatrix} + \varepsilon^2 \begin{bmatrix} N^{(2)} \\ V^{(2)} \\ \phi^{(2)} \end{bmatrix} \\ &+ \varepsilon^3 \begin{bmatrix} N^{(3)} \\ V^{(3)} \\ \phi^{(3)} \end{bmatrix} + \dots \end{aligned} \quad (9)$$

On substituting (8) and (9) into eqs (1)–(7), we obtain the lowest order, i.e.,  $O(\varepsilon)$  as

$$-S\partial_\xi N^{(1)} + \partial_\xi V^{(1)} = 0 \quad (10)$$

$$-S\partial_\xi V^{(1)} = -\partial_\xi \phi^{(1)} - 2\sigma\partial_\xi N^{(1)} \quad (11)$$

$$\alpha_1\phi^{(1)} + \alpha\gamma\phi^{(1)} - (1 - \alpha)N^{(1)} = 0. \quad (12)$$

Solving eqs (10)–(12), we find the following first-order solutions:

$$N^{(1)} = \frac{1}{(S^2 - 2\sigma)}\phi^{(1)} \quad (13)$$

$$V^{(1)} = \frac{S}{(S^2 - 2\sigma)}\phi^{(1)}. \quad (14)$$

On using eqs (13) and (14) in Poisson equation (12) to the lowest-order, i.e.,  $O(\varepsilon)$ , we get the following linear relation for ion-acoustic solitons:

$$S^2 = 2\sigma + \frac{(1 - \alpha)}{(\alpha_1 + \alpha\gamma)}. \quad (15)$$

We obtain the next higher-order from eqs (1) and (7) as

$$-S\partial_\xi N^{(2)} + \partial_\tau N^{(1)} + \partial_\xi(V^{(2)} + N^{(1)}V^{(1)}) = 0 \quad (16)$$

$$\begin{aligned} -S\partial_\xi V^{(2)} + \partial_\tau V^{(1)} + V^{(1)}\partial_\xi V^{(1)} \\ = -\partial_\xi \phi^{(2)} - 2\sigma\partial_\xi N^{(2)} \end{aligned} \quad (17)$$

$$\begin{aligned} \partial_\xi^2\phi^{(1)} &= (\alpha_1 + \alpha\gamma)\phi^{(2)} + \left(\alpha_2 - \frac{\alpha\gamma^2}{2}\right)\phi^{(1)2} \\ &- (1 - \alpha)\frac{1}{(1 - \alpha\varepsilon_Z)}N^{(2)}. \end{aligned} \quad (18)$$

Using eqs (16) and (17), we obtain the following solution:

$$\begin{aligned} \partial_\xi N^{(2)} &= \frac{1}{(S^2 - 2\sigma)} \left[ \frac{2S}{(S^2 - 2\sigma)}\partial_\tau\phi^{(1)} \right. \\ &\left. + \frac{3S^2}{(S^2 - 2\sigma)^2}\phi^{(1)}\partial_\xi\phi^{(1)} + \partial_\xi\phi^{(2)} \right] \end{aligned} \quad (19)$$

Differentiating eq. (18) with respect to  $\xi$

$$\begin{aligned} \partial_\xi^3\phi^{(1)} &= (\alpha_1 + \alpha\gamma)\partial_\xi\phi^{(2)} + \left(\alpha_2 - \frac{\alpha\gamma^2}{2}\right)\partial_\xi\phi^{(1)2} \\ &- (1 - \alpha)\frac{1}{(1 - \alpha\xi_Z)}\partial_\xi N^{(2)} \end{aligned} \quad (20)$$

and using eq. (19) in (20)

$$\begin{aligned} \partial_\xi^3\phi^{(1)} + \left(\frac{3(1 - \alpha)S^2}{(S^2 - 2\sigma)^3} - 2\left(\alpha_2 - \frac{\alpha\gamma^2}{2}\right)\right)\phi^{(1)}\partial_\xi\phi^{(1)} \\ + \frac{2S(1 - \alpha)}{(S^2 - 2\sigma)^2}\partial_\tau\phi^{(1)} = 0 \end{aligned} \quad (21)$$

Solving eq. (21), we obtain the following KdV equation:

$$\partial_\tau\phi^{(1)} + PQ\phi^{(1)}\partial_\xi\phi^{(1)} + \frac{1}{2}P\partial_\xi^3\phi^{(1)} = 0 \quad (22)$$

$$P = \frac{(S^2 - 2\sigma)^2}{S(1 - \alpha)} \quad (23)$$

and

$$Q = \frac{1}{2} \left( \frac{3S^2(1-\alpha)}{(S^2-2\sigma)^3} - 2 \left( \alpha_2 - \frac{\alpha\gamma^2}{2} \right) \right). \tag{24}$$

### 3. Solution of the KdV equation

For the steady-state solution of the KdV equation (22), we consider

$$\eta = \xi - u\tau, \tag{25}$$

where  $u$  is a constant velocity.

Substituting eq. (25) in (22) and integrating with respect to  $\eta$ , we obtain

$$\frac{1}{2} (d_\zeta \phi)^2 + V(\phi) = 0, \tag{26}$$

where  $\phi$  is used in place of  $\phi^{(1)}$  for convenience and  $V(\phi)$  is the Sagdeev potential (SP), which is given by

$$V(\phi) = \frac{2}{P} \left( \frac{1}{6} P Q \phi^3 - \frac{1}{2} u \phi^2 \right). \tag{27}$$

In the derivation of eq. (27), we have used the following boundary conditions: As  $\zeta \rightarrow \pm\infty$ ,  $\phi, d_\zeta \phi$  and  $d_\zeta^2 \phi \rightarrow 0$ . However, for the soliton solution,  $V(\phi)$  should be negative between  $\phi = 0$  and  $\phi = \phi_m$ , where

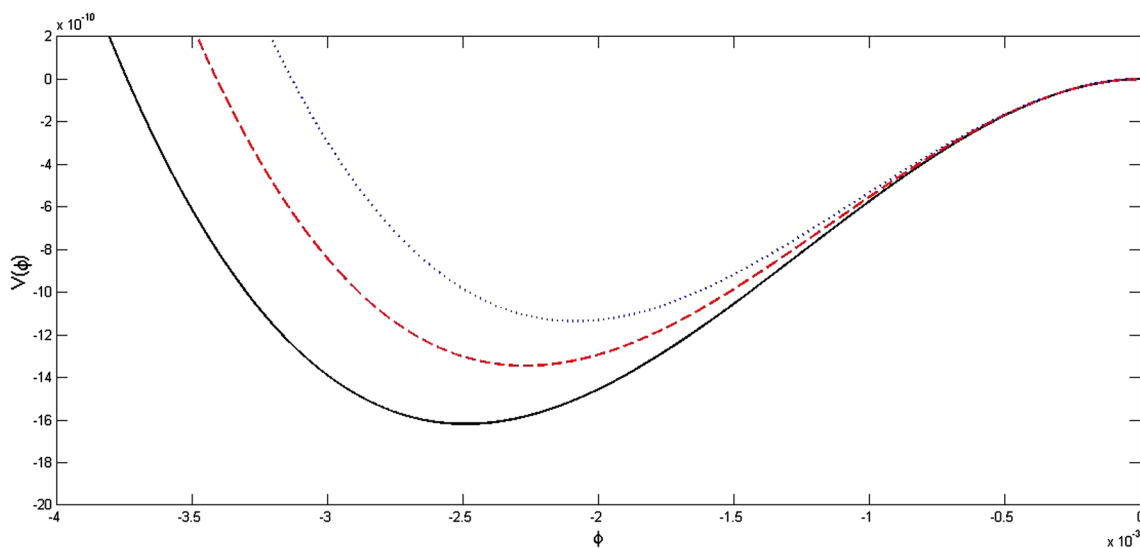


**Figure 1.** The variation of  $V(\phi)$  for the rarefactive soliton when  $k_h = 6.685$  (black solid line),  $6.687$  (red dashed line) and  $6.689$  (blue dotted line) when  $\alpha = 0.1, k_c = 2, \sigma = 0.1, \gamma = 0.7, \sigma_1 = 0.1, \nu = 0.01$  and constant velocity ( $u$ ) =  $0.01$ .

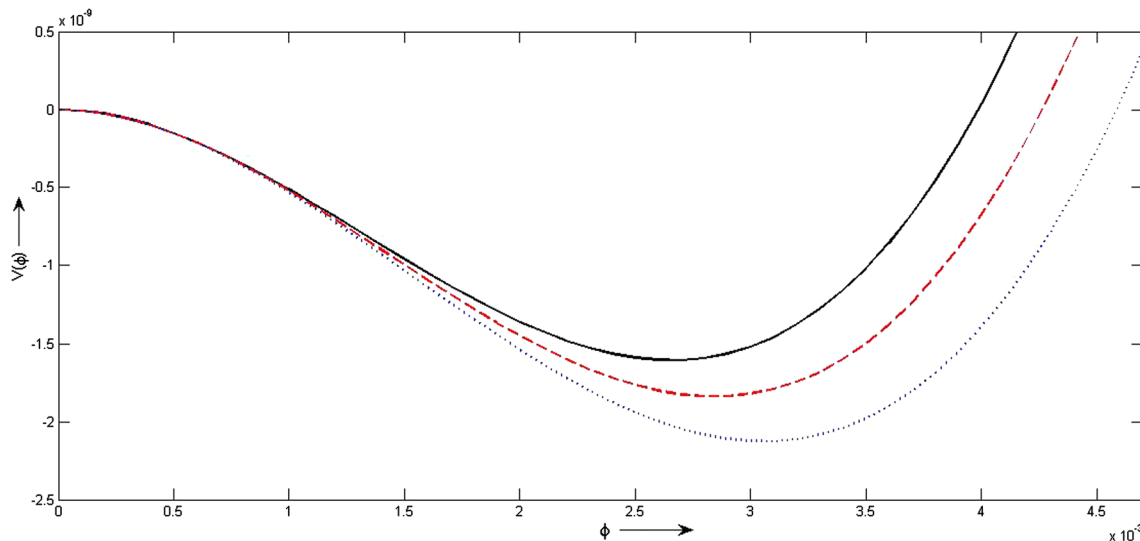


**Figure 2.** The variation of  $V(\phi)$  for the compressive soliton when  $k_h = 6.90$  (black solid line),  $6.91$  (red dashed line) and  $6.92$  (blue dotted line) when  $\alpha = 0.1, k_c = 3, \sigma = 0.1, \gamma = 0.1, \sigma_1 = 0.1, \nu = 0.01$  and constant velocity ( $u$ ) =  $0.01$ .

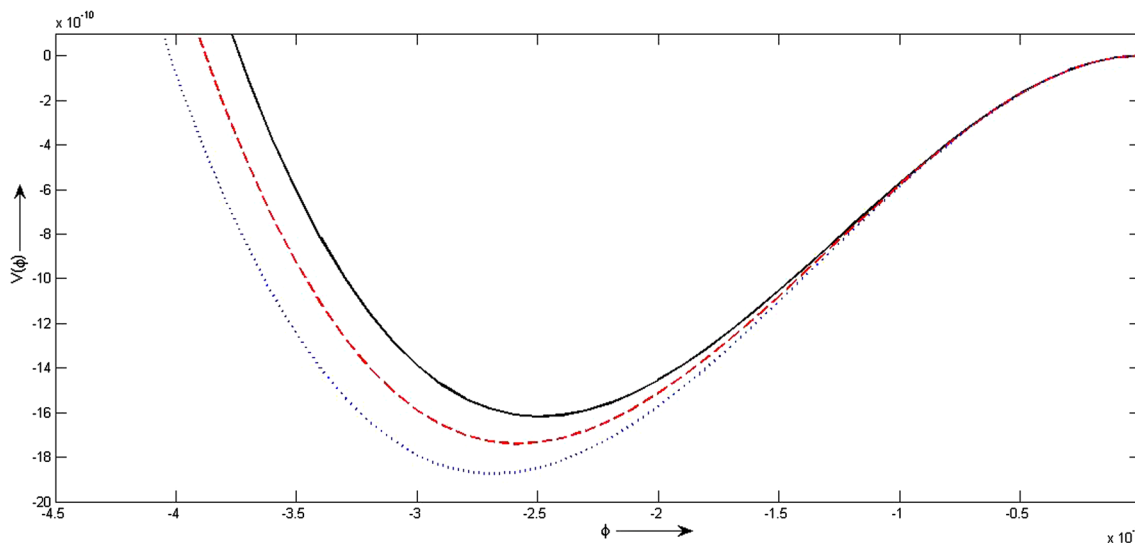


**Figure 3.** The variation of  $V(\phi)$  for the rarefactive soliton when  $k_c = 2.0$  (black solid line),  $2.001$  (red dashed line) and  $2.002$  (blue dotted line) when  $\alpha = 0.1, k_h = 6.685, \sigma = 0.1, \gamma = 0.1, \sigma_1 = 0.1, \nu = 0.01$  and constant velocity ( $u$ ) =  $0.01$ .

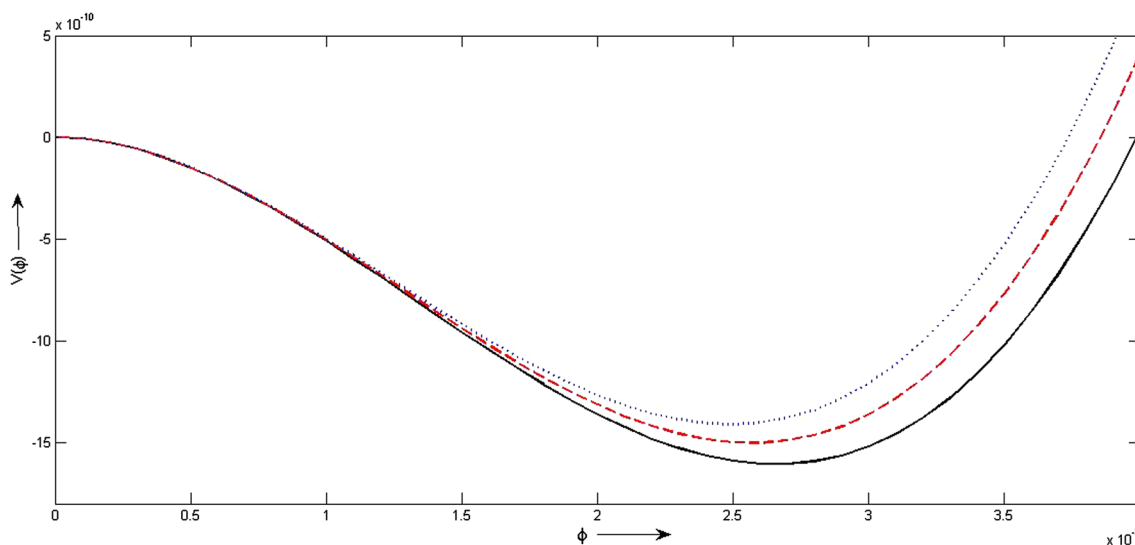


**Figure 4.** The variation of  $V(\phi)$  for the compressive soliton when  $k_c = 3.0$  (black solid line),  $3.01$  (red dashed line) and  $3.02$  (blue dotted line) when  $\alpha = 0.1, k_h = 6.9, \sigma = 0.1, \gamma = 0.1, \sigma_1 = 0.1, \nu = 0.01$  and constant velocity ( $u$ ) =  $0.01$ .

$\phi_m$  is some maximum or minimum value of potential for the compressive and rarefactive solitons, respectively. The following boundary conditions on the SP should be satisfied:

$$V(\phi) = 0 \text{ at } \phi = 0 \text{ and } \phi = \phi_m, \tag{28a}$$

$$V'(\phi) = 0 \text{ at } \phi = 0, \tag{28b}$$

$$V'(\phi) > 0 \text{ at } \phi = \phi_m \text{ for compressive soliton,} \tag{28c}$$

$$V'(\phi) < 0 \text{ at } \phi = \phi_m \text{ for rarefactive soliton.} \tag{28d}$$

The soliton solution of eq. (26) is given by

$$\phi = \phi_m \operatorname{sech}^2[W^{-1}(\xi - u\tau)], \tag{29}$$

where the amplitude ( $\phi_m$ ) and width ( $W$ ) are given by

$$\phi_m = \frac{3u}{PQ} \tag{30}$$

and

$$W = \sqrt{\frac{2P}{u}}. \tag{31}$$

#### 4. Derivation of the m-KdV equation

In the case of two-electron temperature distribution, the nonlinear coefficient in the KdV equation may vanish

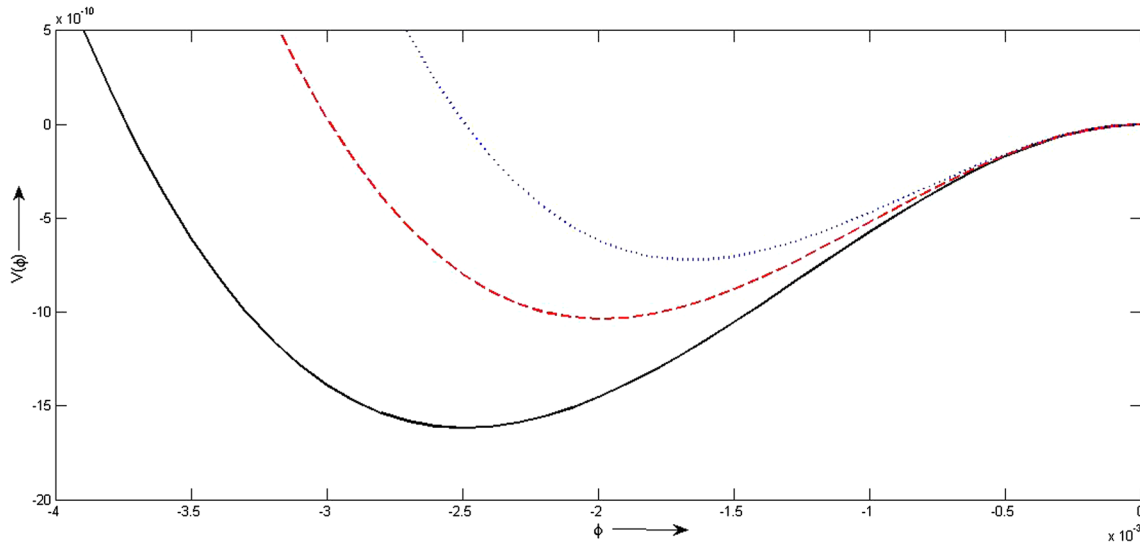


**Figure 5.** The variation of  $V(\phi)$  for the rarefactive soliton when  $\gamma = 0.1$  (black solid line), 0.101 (red dashed line) and 0.102 (blue dotted line) when  $\alpha = 0.1, k_h = 6.685, \sigma = 0.1, \nu = 0.01, \sigma_1 = 0.1, k_c = 2$  and constant velocity ( $u$ ) = 0.01.

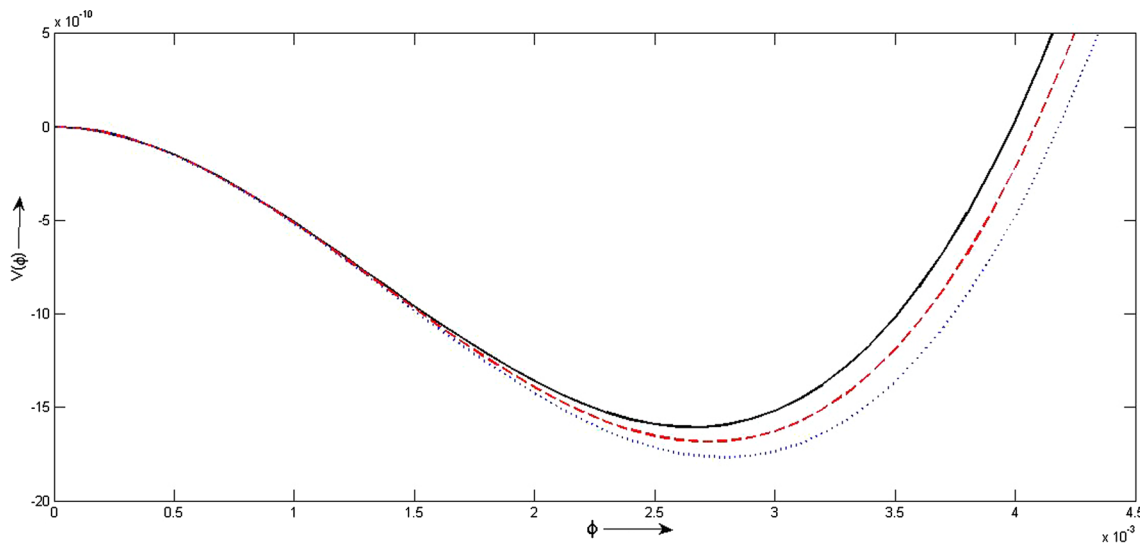


**Figure 6.** The variation of  $V(\phi)$  for the compressive soliton when  $\gamma = 0.1$  (black solid line), 0.101 (red dashed line) and 0.102 (blue dotted line) when  $\alpha = 0.1, k_h = 6.9, \sigma = 0.1, \nu = 0.1, \sigma_1 = 0.1, k_c = 3$  and constant velocity ( $u$ ) = 0.01.

for certain density and temperature ratios of the two-electron species defined as critical density and critical temperature. In the vicinity of this critical regime, the higher-order nonlinearity should be taken into account to obtain the m-KdV equation. To derive the m-KdV equation, we take the stretching of coordinates ( $\xi$ ) and ( $\tau$ ) in the following form:

$$\xi = \varepsilon(x - St) \tag{32a}$$

and

$$\tau = \varepsilon^3 t. \tag{32b}$$

On substituting expansion (32) into eqs (1)–(5) and (7), using eq. (9) and equating terms with the same power of  $\varepsilon$ , we obtain a set of equations for each order in  $\varepsilon$ . The

set of equations for the lowest order, i.e.,  $O(\varepsilon^2)$ , for eqs (1)–(7), and  $O(\varepsilon)$  for eq. (7) comes out to be the same as in the case of the KdV equation. Hence, once again we get the same first-order relations and the dispersion relation.

The next higher-order equations give the following m-KdV equation:

$$\partial_\tau \phi^{(1)} + P R \phi^{(1)2} \partial_\xi \phi^{(1)} + \frac{1}{2} P \partial_\xi^3 \phi^{(1)} = 0, \tag{33}$$

where

$$P = \frac{(S^2 - 2\sigma^2)^2}{S(1 - \alpha)} \tag{34}$$

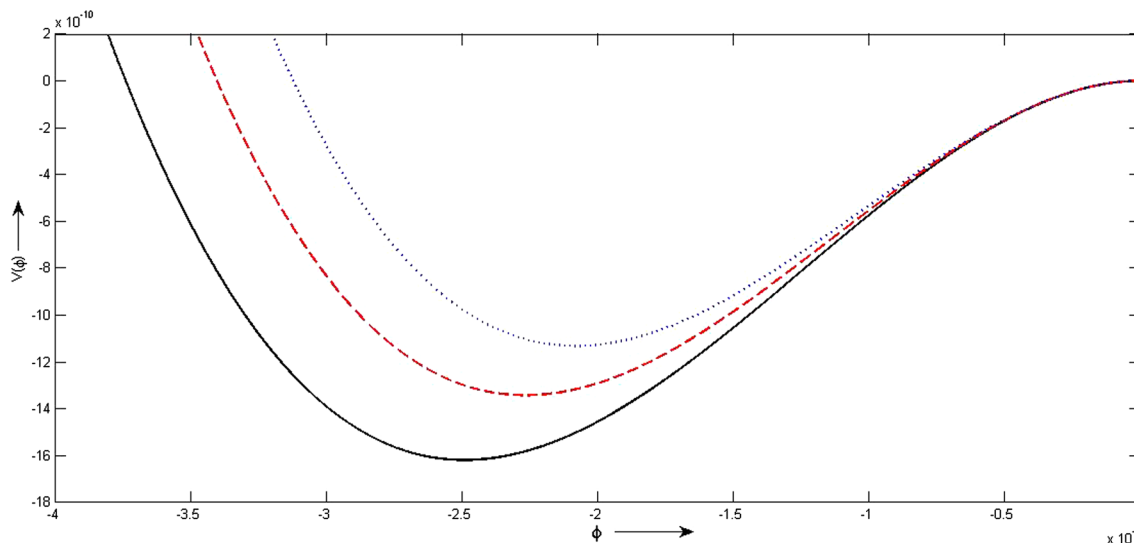


**Figure 7.** The variation of  $V(\phi)$  for the rarefactive soliton when  $\alpha = 0.1$  (black solid line), 0.1003 (red dashed line) and 0.01006 (blue dotted line) when  $\nu = 0.01, k_h = 6.685, \sigma = 0.1, \gamma = 0.1, \sigma_1 = 0.1, k_c = 2$  and constant velocity ( $u$ ) = 0.01.

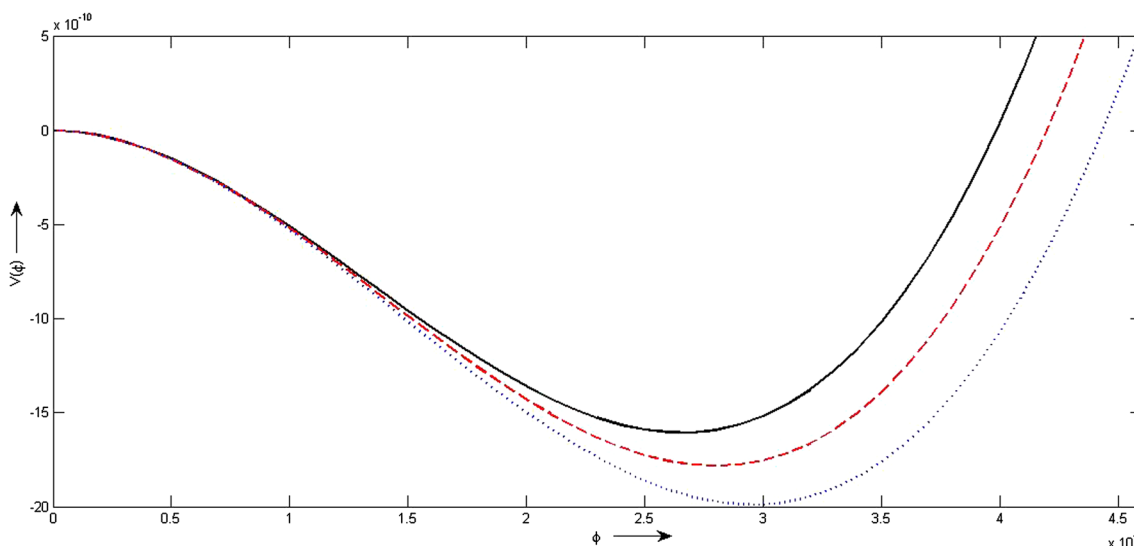


**Figure 8.** The variation of  $V(\phi)$  for the compressive soliton when  $\alpha = 0.1$  (black solid line), 0.1001 (red dashed line) and 0.1002 (blue dotted line) at  $\nu = 0.01, k_h = 6.9, \sigma = 0.1, \gamma = 0.1, \sigma_1 = 0.1, k_c = 3$  and constant velocity ( $u$ ) = 0.01.

and

$$R = \left( \frac{\alpha\gamma^3}{6} - \frac{(1-\alpha)}{2(S^2 - 2\sigma)^5} \left\{ 3S^5 - 3(2\sigma - 1)S^3 + 2S^4 - 4\sigma S^2 \right\} \right). \tag{35}$$

For the steady-state solution of the m-KdV equation (33), we consider the same transformation as used in the KdV soliton case, i.e., eq. (25), and we get

$$\frac{1}{2}(d_\xi\phi)^2 + V(\phi) = 0, \tag{36}$$

where  $V(\phi)$  is the SP, which is given by

$$V(\phi) = \frac{1}{P} \left( \frac{1}{12} PR\phi^4 - \frac{1}{2}u\phi^2 \right). \tag{37}$$

The solution of eq. (36) is given by

$$\phi = \phi_m \operatorname{sech} [W^{-1}(\xi - u\tau)], \tag{38}$$

where the amplitude ( $\phi_m$ ) and width ( $W$ ) are given by

$$\phi_m = \pm \left[ \frac{6u}{PR} \right]^{1/2} \tag{39}$$



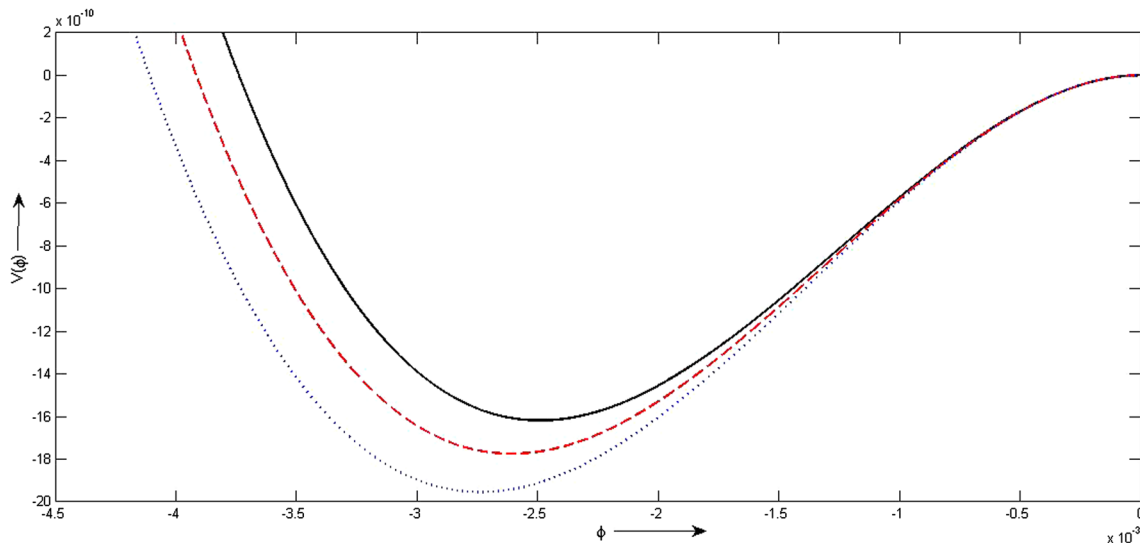


**Figure 9.** The variation of  $V(\phi)$  for the rarefactive soliton when  $\sigma = 0.1$  (black solid line), 0.1001 (red dashed line) and 0.1003 (blue dotted line) when  $\nu = 0.01$ ,  $k_h = 6.685$ ,  $\alpha = 0.1$ ,  $\gamma = 0.1$ ,  $\sigma_1 = 0.1$ ,  $k_c = 2$  and constant velocity ( $u$ ) = 0.01.

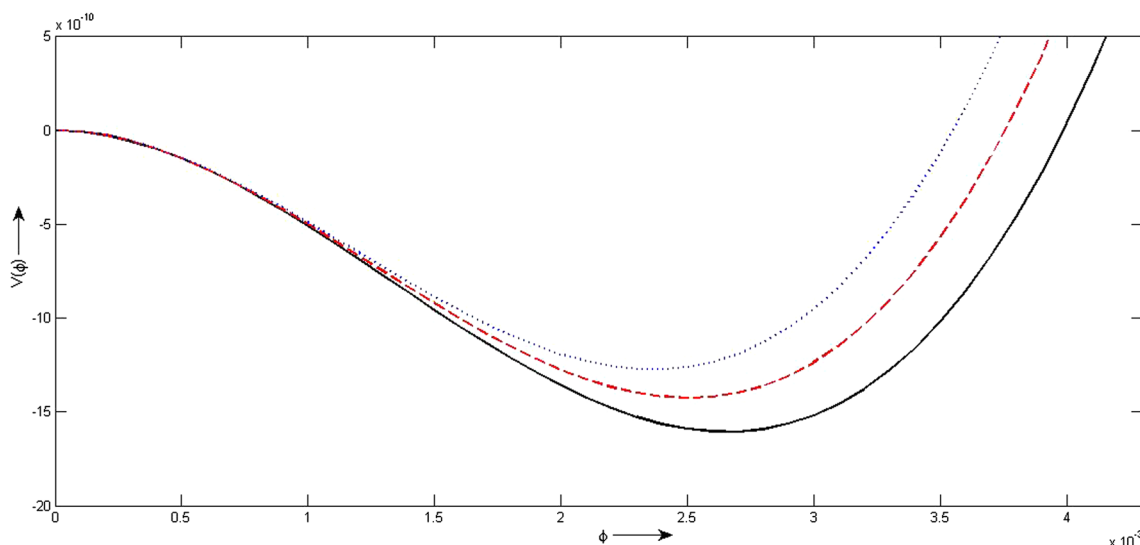


**Figure 10.** The variation of  $V(\phi)$  for the compressive soliton when  $\sigma = 0.1$  (black solid line), 0.101 (red dashed line) and 0.102 (blue dotted line) when  $\nu = 0.01$ ,  $k_h = 6.9$ ,  $\alpha = 0.1$ ,  $\gamma = 0.1$ ,  $\sigma_1 = 0.1$ ,  $k_c = 3$  and constant velocity ( $u$ ) = 0.01.

and

$$W = \sqrt{\frac{P}{2u}}. \tag{40}$$

### 5. Result and discussion

To investigate region of existence of the solitons, their nature, amplitude and width in the plasmas with two species of superthermal electrons, we have numerically

analysed and plotted the valuation of  $V(\phi)$  with potential ( $\phi$ ) for different sets of plasma parameters.

Figures 1–10, 11–12 and 13–15 are drawn using eq. (27), (29) and (31) respectively. In figure 1, the variation of  $V(\phi)$  with  $\phi$  is plotted for rarefactive soliton for different values of  $k_h$  with fixed values of other parameters. It is seen that as  $k_h$  increases, the amplitude of the soliton decreases. In figure 2, the variation of  $V(\phi)$  with  $\phi$  for the compressive soliton is shown for different values of  $k_h$  when  $k_c = 3$  and  $\gamma = 0.1$  (other parameters are the same as in figure 1). It is observed that as  $k_h$  increases, the amplitude of the soliton increases. In figure 3, the



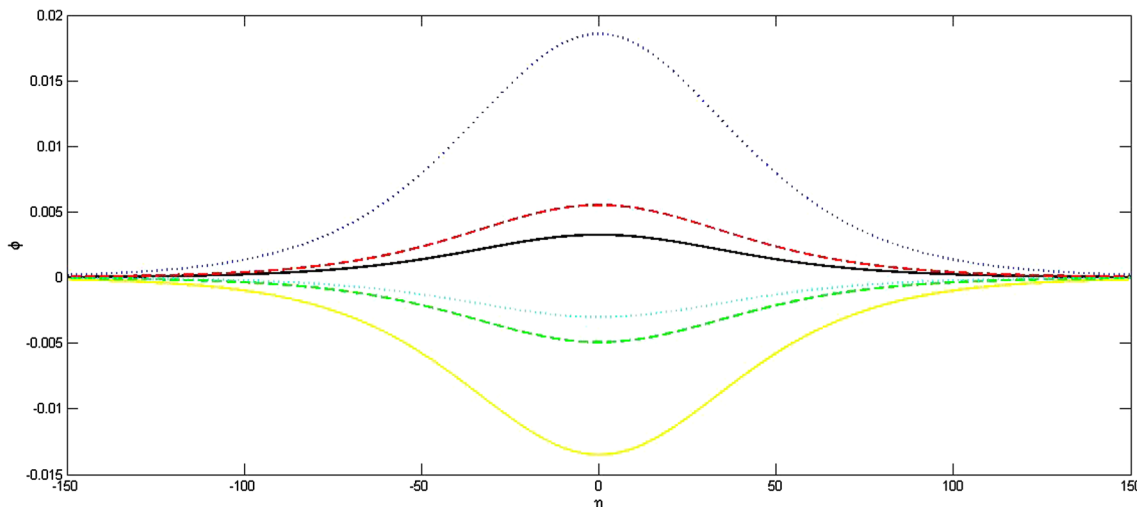


**Figure 11.** The variation of  $\phi$  with  $\eta$  when  $k_h = 6.64$  (black solid line),  $6.65$  (red dashed line),  $6.66$  (blue dotted line),  $6.67$  (yellow solid line),  $6.68$  (green dashed line) and  $6.69$  (cyan dotted line) when  $\nu = 0.01, \sigma = 0.1, \alpha = 0.1, \gamma = 0.1, u = 0.01, \sigma_1 = 0.1$  and  $k_c = 2$ .

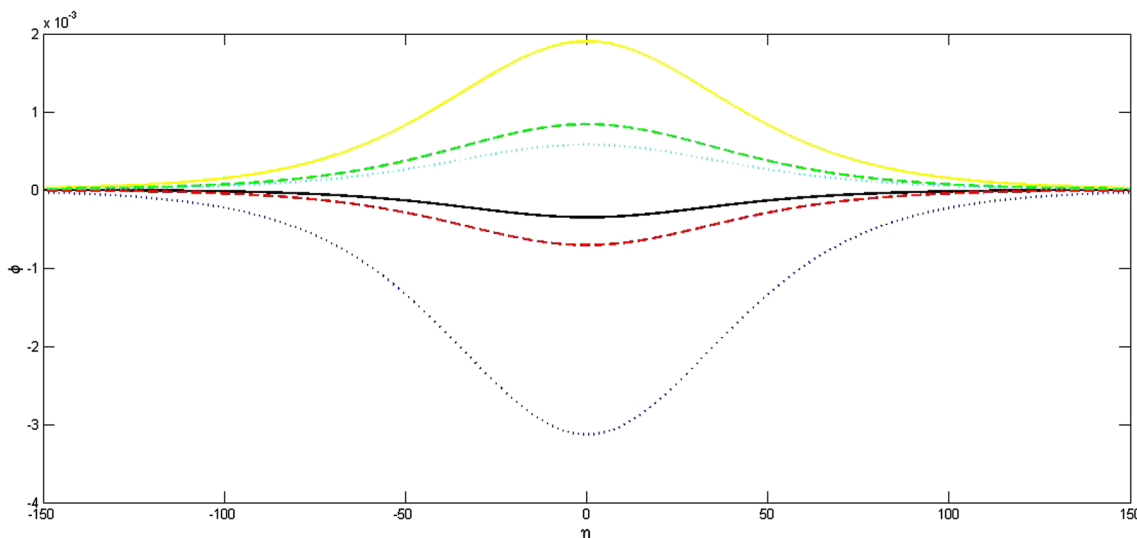


**Figure 12.** The variation of  $\phi$  with  $\eta$  when  $k_c = 1.8$  (black solid line),  $1.9$  (red dashed line),  $2.0$  (blue dotted line),  $2.1$  (yellow solid line),  $2.2$  (green dashed line) and  $2.3$  (cyan dotted line) when  $\nu = 0.01, \sigma = 0.1, \alpha = 0.1, \gamma = 0.1, u = 0.01, \sigma_1 = 0.1$  and  $k_h = 6.689$ .

variation of  $V(\phi)$  with  $\phi$  for the rarefactive soliton is shown for different values of  $k_c$  when  $k_h = 6.685$  and  $\gamma = 0.1$  (other parameters are the same as in figure 1). It is seen that as  $k_c$  increases, the amplitude of the soliton increases. In figure 4, the variation of  $V(\phi)$  with  $\phi$  for the compressive soliton is shown for different values of  $k_c$  when  $k_h = 6.9$  and  $\gamma = 0.1$  (other parameters are the same as in figure 1). It is seen that as  $k_c$  increases, the amplitude of the soliton decreases.

In figure 5, the variation of  $V(\phi)$  with  $\phi$  for the rarefactive soliton is shown for different values of  $\gamma$  when  $k_c = 2$  and  $k_h = 6.685$  (other parameters are

the same as in figure 1). It is seen that as  $\gamma$  increases, the amplitude of the soliton decreases. In figure 6, the variation of  $V(\phi)$  with  $\phi$  for the compressive soliton is shown for different values of  $\gamma$  when  $k_c = 3$  and  $k_h = 6.9$  (other parameters are the same as in figure 1). It is seen that as  $\gamma$  increases, the amplitude of the soliton increases. In figure 7, the variation of  $V(\phi)$  with  $\phi$  for the rarefactive soliton is shown for different values of  $\alpha$  when  $\gamma = 0.1$  and  $k_h = 6.685$  (other parameters are the same as in figure 1). It is seen that as  $\alpha$  increases, the amplitude of the soliton decreases. In figure 8, the variation of  $V(\phi)$  with  $\phi$  for the compressive soliton

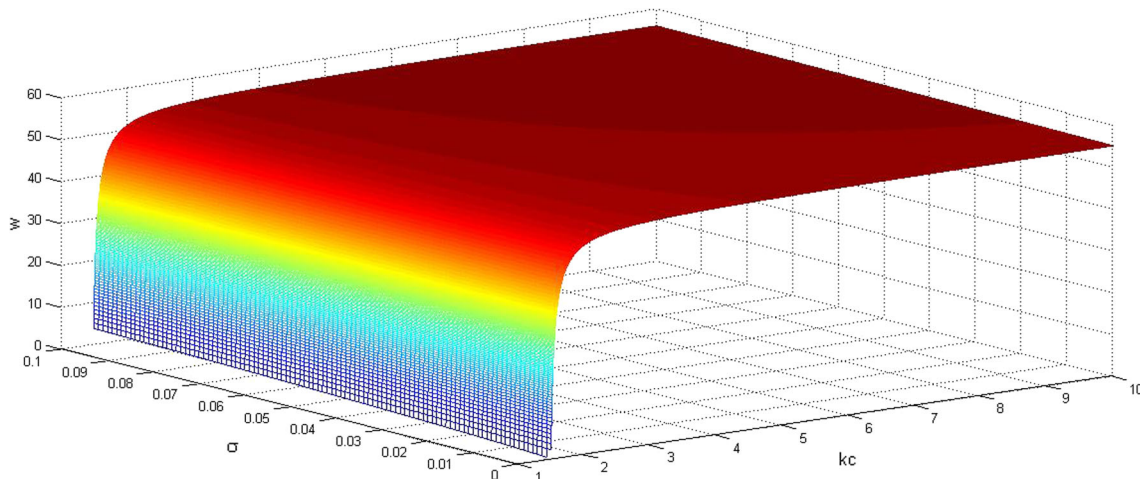


Figure 13. 3D curve between  $k_c$ ,  $\sigma$  and width ( $w$ ) when  $\nu = 0.01$ ,  $\alpha = 0.1$ ,  $\gamma = 0.1$ ,  $\sigma_1 = 0.1$ ,  $u = 0.01$  and  $k_h = 7$ .

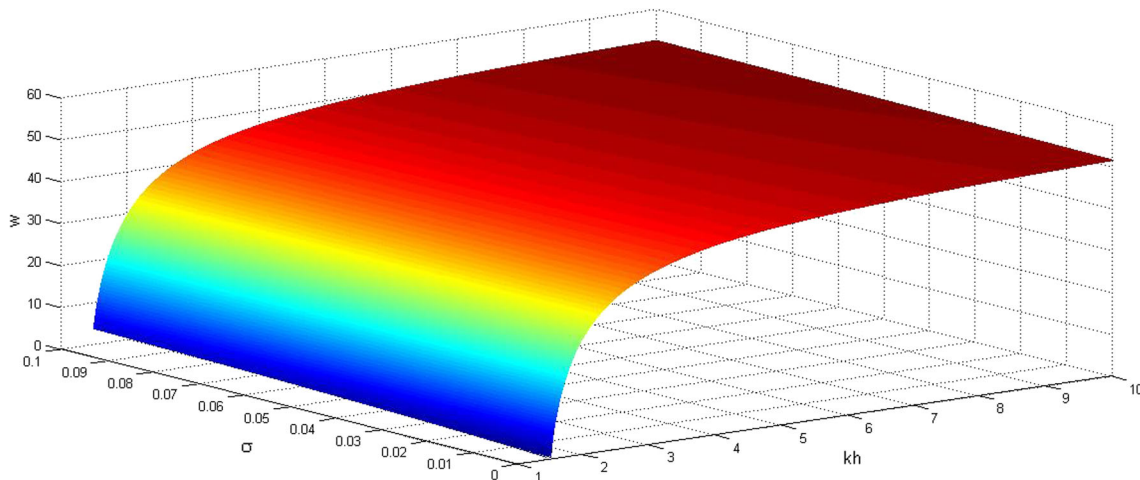


Figure 14. 3D curve between  $k_h$ ,  $\sigma$  and  $w$  when  $\nu = 0.01$ ,  $\alpha = 0.1$ ,  $\gamma = 0.1$ ,  $\sigma_1 = 0.1$ ,  $u = 0.01$  and  $k_c = 2$ .

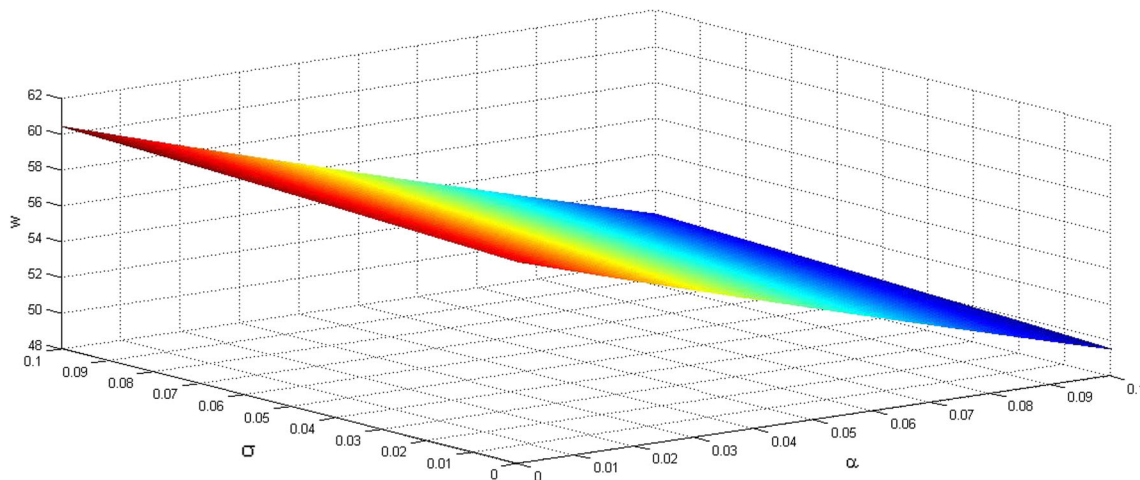


Figure 15. 3D curve between  $\alpha$ ,  $\sigma$  and  $w$  when  $\nu = 0.01$ ,  $k_c = 2$ ,  $\gamma = 0.1$ ,  $\sigma_1 = 0.1$ ,  $u = 0.01$  and  $k_h = 6.689$ .

**Table 1.** The amplitude (eq. (39)) and width (eq. (40)) of m-KdV soliton when  $\sigma = 0.1$ ,  $\alpha = 0.1$ ,  $\nu = 0.01$ ,  $k_c = 6$ ,  $\gamma = 0.1$ ,  $\sigma_1 = 0.1$  and  $u = 0.01$  for different values of  $k_h$ .

$k_h$	Amplitude $ \phi_m $	Width ( $w$ )
1.5	0.0616	0.0181
1.501	0.0669	0.0188
1.502	0.0723	0.0194
1.503	0.0799	0.0201

**Table 2.** The amplitude and width of m-KdV soliton for different values of  $\sigma$  when  $k_c = k_h = 1.5$ . The other parameters are the same as in table 1.

$\sigma$	Amplitude $ \phi_m $	Width ( $w$ )
0.01	0.0074	0.0035
0.02	0.0192	0.0059
0.03	0.0289	0.0079
0.04	0.0490	0.0097

is shown for different values of  $\alpha$  when  $k_c = 3$  and  $k_h = 6.9$  (other parameters are the same as in figure 1). It is seen that as  $\alpha$  increases, the amplitude of the soliton increases. In figure 9, the variation of  $V(\phi)$  with  $\phi$  for the rarefactive soliton is shown for different values of  $\sigma$  when  $k_c = 2$ ,  $\gamma = 0.1$  and  $k_h = 6.685$  (other parameters are the same as in figure 1). It is seen that as  $\sigma$  increases, the amplitude of the soliton increases. In figure 10, the variation of  $V(\phi)$  with  $\phi$  for the compressive soliton is shown for different values of  $\sigma$  when  $k_c = 2$  (other parameters are the same as in figure 1). It is seen that as  $\sigma$  increases, the amplitude of the soliton decreases.

In figures 11 and 12 the variation of  $\phi$  with  $\eta$  (eq. (29)) for different values  $k_h$  and  $k_c$  when  $\gamma = 0.1$  are plotted and other parameters are the same as in figure 1. In figure 13, the 3D curve shows that as  $\sigma$  increases, the width of the soliton increases and as  $k_c$  increases, the width of the soliton increases and after a certain value, there is no change in the width of the plasma. In figure 14, the 3D curve shows that as  $\sigma$  increases, the width of the soliton increases and as  $k_h$  increases, the width of the soliton increases and after a certain value, there is no change in the width of the plasma. In figure 15, the 3D curve shows that as  $\alpha$  increases, the width of the soliton decreases and as  $\sigma$  increases, the width of the soliton increases.

In tables 1 and 2, we have presented the variation in amplitude and width of the m-KdV soliton with the spectral index ( $k_h$ ) and ionic temperature ratio ( $\sigma$ ). It can be seen from tables 1 and 2 that on increasing the values of  $k_h$  and  $\sigma$ , the amplitude as well as the width of the m-KdV soliton increase.

## 6. Conclusions

IASWs have been investigated in the presence of  $\kappa$ -distributed hot and cold electrons, positrons and ions. Employing the RPM, the KdV and m-KdV equations have been derived for the ion-acoustic waves. We have focussed our investigation on the effect of  $\alpha$ ,  $\gamma$ ,  $\sigma$ ,  $k_h$  and  $k_c$  on the characteristics of solitons in unmagnetised plasma. For a selected set of plasma parameters, it is found that on increasing the value of  $\alpha$ ,  $\gamma$  and  $k_h$  the amplitude of the rarefactive (compressive) solitary wave decreases (increases). However, the amplitude increases (decreases) with an increase in  $\sigma$  and  $k_c$  as can be seen in figures 1–10. Width of the solitary wave increases as values of  $\sigma$ ,  $k_h$  and  $k_c$  increase for a given set of parameters as shown in figures 13 to 15. It is predicted that for the selected set of parameters, on increasing  $\alpha$  the width of the solitary wave decreases as shown in figure 15. In the case of m-KdV soliton, it is found that for the selected set of plasma parameters, the amplitude and width of the solitary wave increase with an increase in  $\sigma$  and  $k_h$ . The results of the present investigation may be helpful to understand the nonlinear ion-acoustic soliton in space plasma environments as well as in laboratory plasma, where superthermal electrons with two different temperatures exist along with positrons and ions (e.g. Saturn’s magnetosphere, pulsar magnetosphere) etc.).

## References

[1] R E Ergun *et al*, *Geophys. Res. Lett.* **25**, 2041 (1998)

- [2] L Anderson *et al*, *Phys. Rev. Lett.* **102**, 225004 (2009)
- [3] H Matusmoto, X H Deng, H Kojima and R R Anderson, *Geophys. Res. Lett.* **30**, 1326 (2003)
- [4] L B Wilson III, C Cattell, P J Kellogg, K Geotz, K Kersten, L Hanson, R MacGregor and J C Kapsner, *Phys. Rev. Lett.* **99**, 041101 (2007)
- [5] B Lefebvre, L Chen, W Gekelman, P Kitner, J Pickett, P Pribyl, S Vincena, F Chiang and J Judy, *Phys. Rev. Lett.* **105**, 115001 (2010)
- [6] B Buti, *J. Plasma Phys.* **24**, 169 (1980)
- [7] K Nishihara and M Tajiri, *J. Phys. Soc. Jpn.* **50**, 4047 (1981)
- [8] S S Dash and B Buti, *Phys. Lett. A* **81**, 347 (1981)
- [9] O N Krokhin and S P Tsybenko, *Sov. J. Plasma Phys.* **12**, 365 (1986)
- [10] S Baboolal, R Bharuthram and M A Hellberg, *Phys. Fluids B* **2**, 2259 (1990)
- [11] L L Yadav and S R Sharma, *Phys. Lett. A* **150**, 397 (1990)
- [12] V K Sayal, L L Yadav and S R Sharma, *Phys. Scr.* **47**, 576 (1993)
- [13] S S Ghosh, K K Ghosh, A N Sekar Iyengar, *Phys. Plasmas* **3**, 3939 (1996)
- [14] M K Mishra, R S Tiwari and S K Jain, *Phys. Rev. E* **76**, 036401 (2007)
- [15] R Bharuthram, E Momoniat, F Mahomed, S V Singh and M K Islam, *Phys. Plasmas* **15**, 082304 (2008)
- [16] T K Baluku and M A Hellberg, *Phys. Plasmas* **19**, 012106 (2012)
- [17] M K Mishra, R S Tiwari and J K Chawla, *Phys. Plasmas* **19**, 062303 (2012)
- [18] S K Jain and M K Mishra, *Astrophys. Space Sci.* **346**, 395 (2013)
- [19] Y Nishida and T Nagasawa, *Phys. Fluids* **29**, 345 (1986)
- [20] V K Sayal and S R Sharma, *Phys. Lett. A* **149**, 155 (1990)
- [21] M M Masud, I Tasnim and A A Mamun, *Pramana – J. Phys.* **84**, 137 (2015)
- [22] P Christon, D G Mitchell, D J Williams, L A Frank, C Y Huang and T E Eastman, *J. Geophys. Res.* **93**, 2562 (1995)
- [23] R A Crains, A A Mamun, R Bingham, R Bostrom, R O Dendy, C M C Naim and P K Shukla, *Geophys. Res. Lett.* **22**, 2709 (1995)
- [24] V Pierrard and J Lemaire, *J. Geophys. Res.* **101**, 7923 (1996)
- [25] O Adriani *et al*, *Nature* **458**, 607 (2009)
- [26] E C Sittler, Jr, K W Ogilive and J D Scudder, *J. Geophys. Res.* **88**, 8847 (1983)
- [27] D D Barbosa and W S Kurth, *J. Geophys. Res.* **98**, 9351 (1993)
- [28] D T Young *et al*, *Science* **307**, 1262 (2005)
- [29] P Schippers *et al*, *J. Geophys. Res.* **113**, A07208 (2008)
- [30] D P Chapagi, J Tamang and A Saha, <https://doi.org/10.1515/zna-2019-0210>
- [31] A Saha and P Chatterjee, *Astrophys. Space Sci.* **163**, 353 (2014)
- [32] M A Hellberg, R L Mace, T K Baluku, I Kourakis and N S Saini, *Phys. Plasmas* **16**, 094701 (2009)
- [33] N Boubakour, M Tribeche and K Aoutou, *Phys. Scr.* **79**, 065503 (2009)
- [34] S A El-Tantawy and W M Moslem, *Phys. Plasmas* **18**, 112105 (2011)
- [35] S A El-Tantawy, N A El-Bedwehy and W M Moslem, *Phys. Plasmas* **18**, 052113 (2011)
- [36] S K El-Labany, R Sabry, E F El-Shamy and D M Khedr, *J. Plasma Phys.* **79**, 613 (2013)
- [37] A Panwar, C M Ryu and A S Bains, *Phys. Plasmas* **21**, 122105 (2014)
- [38] E F El-Shamy, *Phys. Plasmas* **21**, 082110 (2014)
- [39] M S Alam, M M Masaud and A A Mamun, *Astrophys. Space Sci.* **349**, 245 (2014)
- [40] A Saha, N Pal and P Chatterjee, *Phys. Plasmas* **21**, 102101 (2014)
- [41] N S Saini, B S Chahal, A S Bains and C Bedi, *Phys. Plasmas* **21**, 022114 (2014)
- [42] A S Bains, A Panwar and C M Ryu, *Astrophys. Space Sci.* **360**, 17 (2015)
- [43] P Chatterjee, R. Ali and A Saha, <https://doi.org/10.1515/zna-2017-0358>